Journal of The Electrochemical Society, **149** (9) A1250-A1254 (2002)
0013-4651/2002/149(9)/A1250/5/$7.00 © The Electrochemical Society, Inc.

Synthesis and Electrochemical Characteristics of $Li_{0.7}[Ni_{1/6}Mn_{5/6}]O_2$ Cathode Materials

K. S. Park,[a] S. H. Park,[b] Y-K. Sun,[b,*,z] K. S. Nahm,[a,*] C. S. Yoon,[c] C. K. Kim,[c] Yun Sung Lee,[d] and Masaki Yoshio[d,*]

[a]*School of Chemical Engineering and Technology, College of Engineering, Chonbuk National University, Chonju 561-756, Korea*
[b]*Department of Chemical Engineering and* [c]*Division of Materials Science and Engineering, Hanyang University, Seoul 133-791, Korea*
[d]*Department of Applied Chemistry, Saga University, 1 Honjo, Saga 840-8502, Japan*

$Li_{0.7}[Ni_{1/6}Mn_{5/6}]O_2$ powders have been prepared by ion exchange of Li for Na in $Na_{2/3}[Li_{1/6}Mn_{5/6}]O_2$ precursor synthesized by a sol-gel method using glycolic acid as a chelating agent. The material delivers 180 mAh/g and shows excellent cyclability, retaining 98% (0.0486 mAh/g·cycle) of the initial capacity after 50 cycles. The electrochemical behavior and structural transformation of $Li_{0.7}[Ni_{1/6}Mn_{5/6}]O_2$ electrode after cycling was investigated using X-ray diffraction, transmission electron microscopy (TEM), and cyclic voltammetry (CV). Both charge/discharge and CV curves indicate that the $Li_{0.7}[Ni_{1/6}Mn_{5/6}]O_2$ powder has a unique electrochemical property that differs from those of the layered or spinel Li-Mn-O phases. Close examination of the powder structure using TEM revealed that the as-prepared powder consists of a new type of defective spinel structure with a high density of planar faults along a particular crystallographic direction, which appears to be removed by the electrochemical cycling.
 [DOI: 10.1149/1.1501097]

Manuscript submitted August 7, 2001; revised manuscript received March 28, 2002. Available electronically August 6, 2002.

The Li-Mn-O system has generated a great deal of interest as an insertion cathode for rechargeable lithium batteries due to its high energy density, low cost, and low toxicity. Intensive research efforts have been spent on the spinel $LiMn_2O_4$ as the most promising candidate in spite of its lower discharge capacity compared to $LiCoO_2$ and $LiNiO_2$.[1-6] However, a wide use of the spinel material has been limited due to the gradual degradation of its capacity over extended electrochemical cycling. The capacity fading has been attributed to a number of reasons including the spinel particle dissolution in the electrolyte, the Jahn-Teller effect, and lattice instability. Moreover, the $LiMn_2O_4$ electrode shows a poor cycling behavior due to the accelerated Mn dissolution at high temperatures around 50-80°C.[7-9]

As an alternative Li-Mn-O material to the spinel $LiMn_2O_4$, the $LiMnO_2$ layered structure has been actively studied due to its high theoretical discharge capacity of 285 mAh/g, which is nearly twice that of spinel $LiMn_2O_4$. To harness such large discharge capacity of the $LiMnO_2$, many research groups have attempted to prepare monoclinic $LiMnO_2$ (m-$LiMnO_2$) with the O3 (α-$NaFeO_2$) structure and orthorhombic $LiMnO_2$ (o-$LiMnO_2$). However, both the m- and o-$LiMnO_2$ were observed to undergo a detrimental phase transformation to a spinel-like phase through minor atomic rearrangements during the first removal and subsequent cycling of Li, leading to eventual degradation of electrode performance.[10-17]

Recently, Paulsen *et al.* reported that the high-temperature O2-type $Li_{0.7}[Ni_{1/3}Mn_{2/3}]O_2$ prepared by ion exchange Li for Na from the P2-type $Na_{0.7}[Ni_{1/3}Mn_{2/3}]O_2$ showed a large capacity of about 180 mAh/g, good capacity retention, and did not convert to spinel on cycling.[18-20] In order to further stabilize the layer structure, many research groups have studied the Mn-substituted $Li_xM_yMn_{1-y}O_2$ (M = Al, Cr, Co, Ni, Li, Ti, Mg).[15-19,21] Quine *et al.* reported that although m-$Li_xMn_{0.95}Ni_{0.05}O_2$ prepared by ion-exchanging of $NaMn_{0.95}Ni_{0.05}O_2$ delivered a reversible capacity retention of 220 mAh/g between 4.8 and 2.4 V, showing good capacity retention after 50 cycles, the material transformed slowly to a spinel-like material during cycling.[22] $LiCr_xMn_{1-x}O_2$ cathodes with low-level substitution prepared by solid-state reaction showed a minimal degree of phase transformation to a spinel-type structure during cycling between 4.4 and 2.0 V and maintained the initial hexagonal structure.[23]

In this work, we have attempted to synthesize a layered structure, $Li_{0.7}[Ni_{1/6}Mn_{5/6}]O_2$, through ion exchange of Li for Na from the $Na_{0.7}[Ni_{1/6}Mn_{5/6}]O_2$ precursor which was prepared by a sol-gel method. In the process, we have fortuitously discovered a new defective spinel structure whose chemical formula is likely to be $Li_{1.4}Ni_{1/3}Mn_{5/3}O_4$ and, more importantly, the material does not show the noticeable capacity fade when cycled from 2.0 to 4.6 V, typically exhibited by the normal $LiMn_2O_4$. Because it is difficult to clearly distinguish the layered structures (especially, m-$LiMnO_2$) after ion exchange from the spinel phases due to the similarity of X-ray diffraction (XRD) patterns, we have utilized transmission electron microscopy (TEM) to conclusively prove that the initial powder had the new defect spinel structure with unique electrochemical cycling behavior.

Experimental

$Na_{0.7}[Ni_{1/6}Mn_{5/6}]O_2$ precursor was synthesized using a sol-gel method. $NaCH_3COO$, $Ni(CH_3COO)\cdot 4H_2O$, and $Mn(CH_3COO)_2\cdot 4H_2O$ salts with a cationic ratio of Na:Ni:Mn = 0.7:1/6:5/6 were dissolved in distilled water. The dissolved solution was added dropwise to a continuously stirred aqueous solution of glycolic acid as a chelating agent. The molar ratio of chelating agent to total metal ions was fixed in unity. The pH of the solution was adjusted to be in the range of 8-9 by adding ammonium hydroxide. The resultant solution was evaporated at 70-80°C until a transparent sol and gel was obtained. The resulting gel precursors were decomposed at 450°C for 10 h in air, calcined at 800°C in air for 12 h, and then quenched to room temperature.

The prepared precursor, $Na_{0.7}[Ni_{1/6}Mn_{5/6}]O_2$ powders, were introduced into a mixed solution of hexanol and lithium bromide. The ion exchange of Na for $Na_{0.7}[Ni_{1/6}Mn_{5/6}]O_2$ with Li was carried out at 160°C for 3 h in the solution in a batch reactor equipped with a reflux condenser to prepare $Li_{0.7}[Ni_{1/6}Mn_{5/6}]O_2$. After the reaction, the solution was filtered using a vacuum suction filtering equipment and the remaining powder was washed with ethanol. The washed powder was dried at 180°C for 1 day in a vacuum oven.

Powder XRD (Rigaku, Rint-2000) using Cu Kα radiation was used to identify the crystalline phase of the materials. Rietveld refinement was then performed on the XRD data to obtain lattice constants. TEM (JEOL 2010, Japan) was used in conjunction with

* Electrochemical Society Active Member.
z E-mail: yksun@hanyang.ac.kr

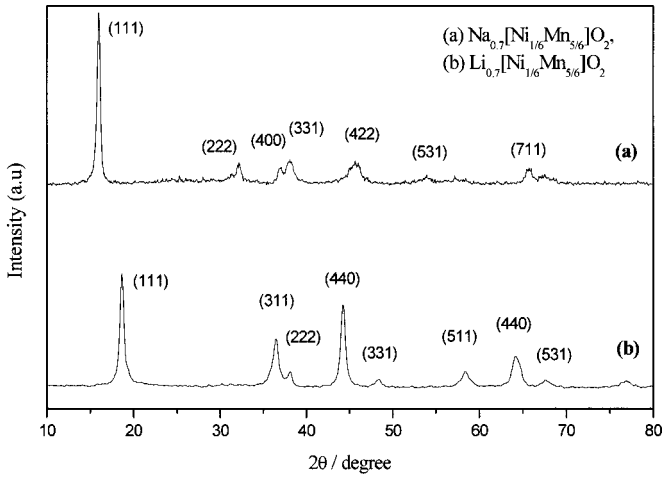

Figure 1. XRD for the as-prepared $Li_{0.7}[Ni_{1/6}Mn_{5/6}]O_2$ powder.

XRD to elucidate the powder structure prior to and after electrochemical cycling.

The electrochemical characterization was carried out using CR2032 coin-type cells. The cell consisted of a cathode and a lithium metal anode separated by a porous polypropylene film. For the fabrication of the electrode, the mixture, which contained 25 mg $Li_{0.7}[Ni_{1/6}Mn_{5/6}]O_2$ powders and 15 mg conducting binder [10 mg Teflonized acetylene black (TAB) and 5 mg graphite], was pressed on 2.0 cm^2 stainless screen at 800 kg/cm^2. The used electrolyte was a 1:2 mixture of ethylene carbonate (EC) and dimethyl carbonate (DMC) containing 1 M $LiPF_6$ by volume. The cell was first charged and discharged at a current density of 0.4 mA/cm^2 with cutoff voltages from 2.0 to 4.2 V (*vs.* Li/Li^+) for three cycles. The upper voltage was sequentially increased by 0.2-4.4 V (3 cycles), and then finally cycled to 4.6 V.

Results and Discussion

Figure 1 shows the XRD pattern of the as-prepared $Li_{0.7}[Ni_{1/6}Mn_{5/6}]O_2$ powder. As can be seen from the indexed XRD pattern, the XRD data closely matches the spinel structure while, it is true that it is difficult to differentiate the spinel structure from the equivalent layered phases. The spinel structure for the as-prepared was rather unexpected since the stable undistorted P2- $Na_{2/3}MnO_2$ phase has been previously reported when the powder was prepared in air at 700°C.[24] It is also observed that the (003) peak ($2\theta = 16°$) from the Na phase has disappeared, indicating that the ion exchange process is complete. Its chemical formula was determined through inductively coupled plasma (ICP) analysis to be

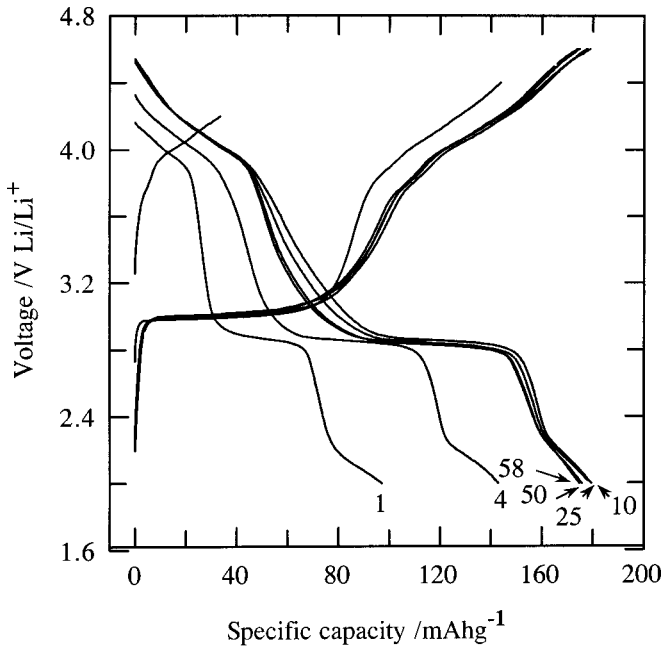

Figure 2. Charge-discharge curves for $Li_{0.7}[Ni_{1/6}Mn_{5/6}]O_2$ cell as a function of cycle number.

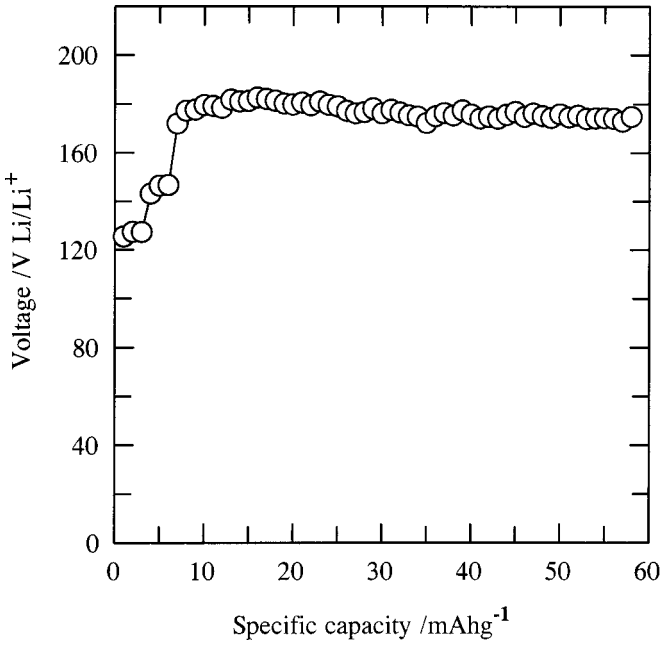

Figure 3. Specific discharge capacity for the Li/ $Li_{0.7}[Ni_{1/6}Mn_{5/6}]O_2$ cell as a function of cycle number.

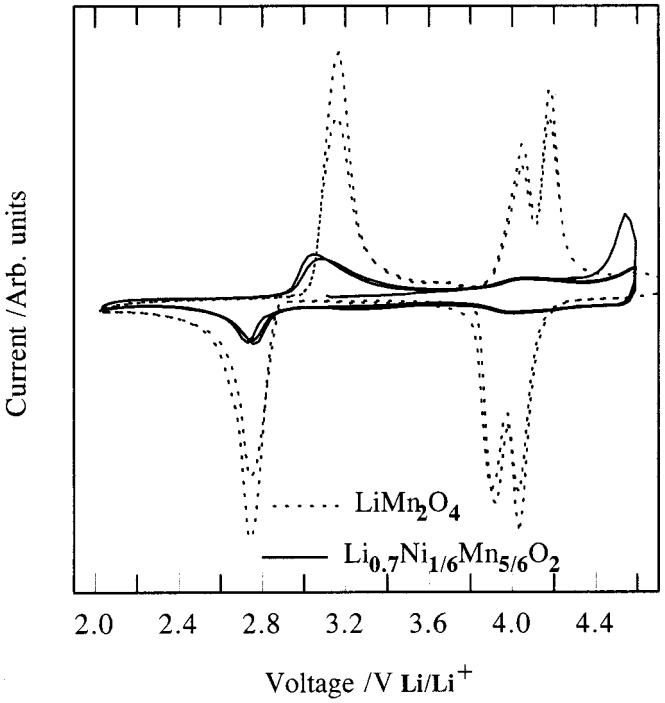

Figure 4. CVs of $Li_{0.7}[Ni_{1/6}Mn_{5/6}]O_2$ electrode at 10 μV/s.

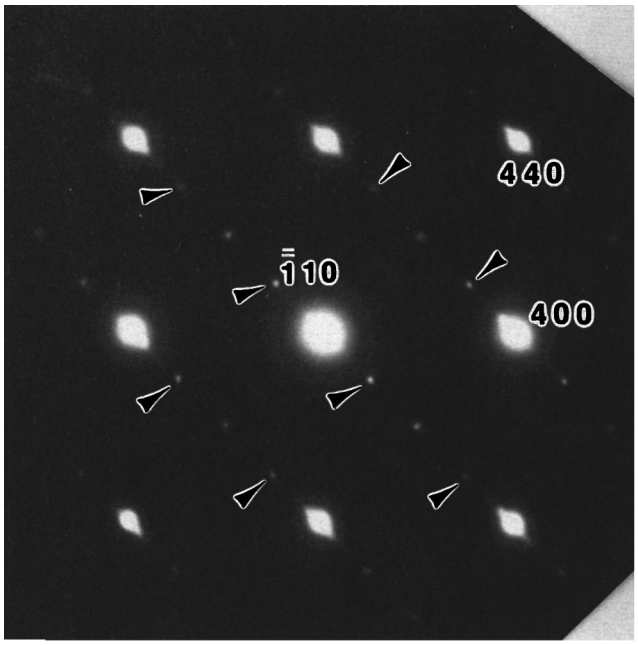

(a)

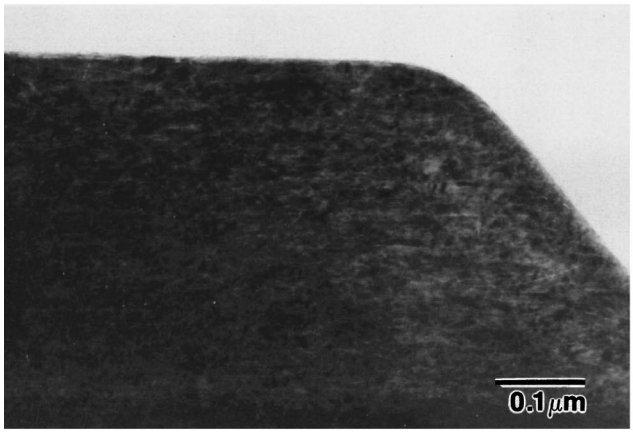

(b)

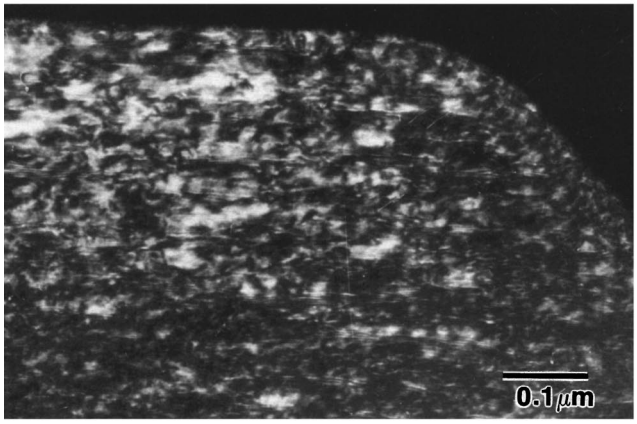

(c)

Figure 5. (a) Electron diffraction pattern of a powder particle before cycling in the [001] zone (spots indicated by arrows are forbidden peaks); (b) bright field TEM image of the as-prepared powder; (c) (400) dark field TEM image of the powder before cycling.

$Li_{0.67}[Ni_{0.17}Mn_{0.83}]O_{2+y}$. The average oxidation state of manganese in the material was 3.53, which was measured by a potentiometric and a back titration method. This value is very similar to theoretical average oxidation state of manganese, which value is 3.57.

Figure 2 shows the charge-discharge curves for the $Li/Li_{0.7}[Ni_{1/6}Mn_{5/6}]O_2$ cell with the corresponding discharge capacity as a function of cycle number shown in Fig. 3. The $Li_{0.7}[Ni_{1/6}Mn_{5/6}]O_2$ electrode initially delivered a charge capacity of 35 and 146 mAh/g during first two cycles when $Li/ Li_{0.7}[Ni_{1/6}Mn_{5/6}]O_2$ cell was cycled between 4.2 and 2.0 V, respectively. The discharge capacity of the electrode subsequently increases with increasing upper voltage and delivers a discharge capacity of 172 mAh/g after seven cycles. When the voltage level was raised to 4.6 V, the electrode showed an excellent cycling behavior, retaining 98% (0.0486 mAh/g · cycle) of the initial capacity after 50 cycles at C/9 rate. Recently, Quine and co-workers reported that layered $Li_xMn_{1-y}Ni_yO_2$ with the O3 (α-$NaFeO_2$) structure delivers a high capacity of 220 mAh/g in the voltage 2.4-4.8 V; however, the cycled electrode transformed to a spinel-like structure after scores of cycling.[22] Although the discharge curve at the first (2.0-4.2 V) and fourth cycle (2.0-4.4 V) shows two distinct plateaus at around 4 and 3 V resembling that observed for a spinel-type manganese oxide structure, the voltage profile after eight cycles (2.0-4.6 V) evolves more structure with distinct inflection in the curve at *ca.* 40 and 140 mAh/g. The middle part of the discharge curve (*e.g.,* 40-100 mAh/g) shifts to lower voltage on subsequent charge-discharge cycling, but the curve retains the distinct inflection. The most important feature in Fig. 2 is that no further capacity change (loss or increase) is observed at all after the initial ten cycles, suggesting that no additional phases are formed in our material during cycling. In addition, the discharge curves at around the 2.8 V region stabilize upon further cycling, and no significant change in the voltage profile of the charging curves is observed.

Shown in Fig. 4 is a slow sweep cyclic voltammogram (CV) of the $Li_{0.7}[Ni_{1/6}Mn_{5/6}]O_2$with a scan rate of 0.1 mV/s between the potential range of 2.0 and 4.6 V. For comparison, a spinel $LiMn_2O_4$ is also presented in Fig. 4. Two pairs of clearly separated oxidation and reduction peaks of the $Li_{0.7}[Ni_{1/6}Mn_{5/6}]O_2$ are observed at 2.75-4.00 and 3.18-4.05 V. In subsequent cycles, the two pairs of oxidation and reduction peaks do not change. The most peculiar characteristics of the CV is the occurrence of a large oxidation peak located at 4.53 V on the first charge, which completely disappeared in subsequent cycles. The areas under the two redox peaks are almost equal. These results indicate that the intercalation/deintercalation of Li ions each occur in two-stage processes and are reversible in this material.

To understand the phase transformation induced by the cycling in detail, the TEM analysis was carried out with the material previously used for the capacity cycle test, where the sample was analyzed in the fully discharged state (2 V). When the as-prepared powder was examined using TEM, the electron diffraction study revealed a fourfold symmetry which none of the layered structures (orthorhombic, monoclinic, O2, O3...) can possess. Further TEM examination together with the XRD data led us to believe that the powder had the spinel structure with a high degree of thin plates of planar faults on the $(\bar{1}10)$ planes, as indicated by the streaks parallel to the $[\bar{1}10]$ direction in the electron diffraction pattern shown in Fig. 5a. The streaks in the diffraction pattern occur due to thin platelets of defects aligned normal to the $[\bar{1}10]$ direction. The forbidden reflections in the face-centered cubic (fcc) spinel structure also can be seen in the electron diffraction pattern. Shown in Fig. 5b and c are the corresponding bright and (400) dark field images of the as-prepared powder particle, which do not show typical stacking fault contrast. Instead, as can be clearly seen from the dark field image, the particle appears to be composed of highly faulted elongated domains. We have found that all the particles examined in the [001] zone showed similar diffraction patterns and images. The pla-

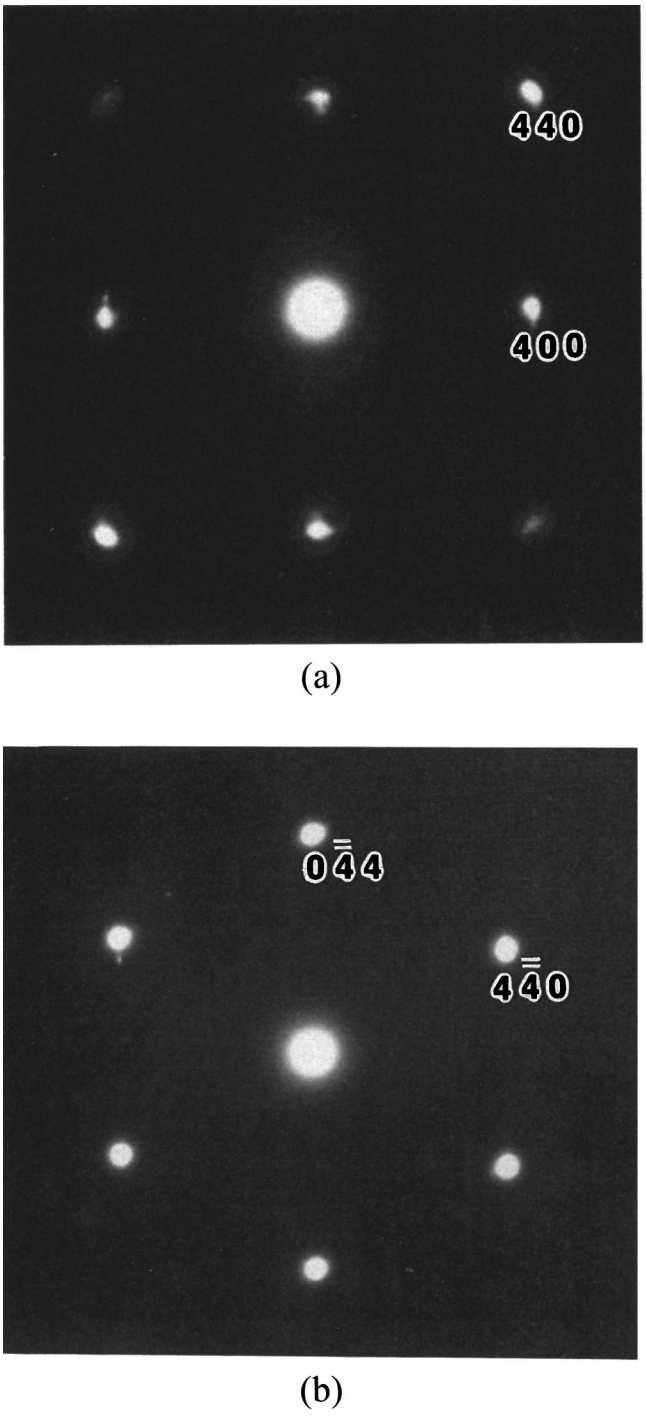

Figure 6. (a) Electron diffraction pattern of a powder particle after cycling in the [001] zone; (b) diffraction pattern of a different particle in the [111] zone.

nar faults seen in the diffraction pattern could have arisen from the wrong stacking sequence along the $[\bar{1}10]$ direction; however, the spinel with fcc structure forms its stacking fault in the [111] closed-packed direction. Moreover, the presence of the $(\bar{1}10)$ reflection and the disordered appearance in the bright and dark field image suggest that the fault is related to the breakdown of symmetry among {110} planes, leading to the generation of the forbidden diffraction peaks. $LiMn_2O_4$ has been previously doped with Ni up to $LiNi_{0.5}Mn_{1.5}O_4$.[5] Similar to our material, $LiNi_{0.5}Mn_{1.5}O_4$ did suppress the Jahn-Teller distortion due to the doped divalent Ni but showed a different electrochemical cycling behavior with gradual decrease in the discharge capacity. No such faulted structure was reported in the $LiNi_{0.5}Mn_{1.5}O_4$ material. The Ni doping alone does not seem to be responsible for producing the distorted spinel-like structure; it appears that the disorder in the (110) plane could have come from the rearrangement of atoms in the plane due to the nonstoichiometry of Li and Ni doping during the ion-exchange process.

Figure 6 shows the electron diffraction patterns of two different particles after cycling taken along different zones. As can be seen, the diffraction patterns in [001] and [111] zones no longer show the streaks and forbidden reflections associated with the structural distortion. The electrochemical cycling appears to have improved the crystallinity of the material, removing the planar faults on the (110) plane. The inflection in the discharge curve in Fig. 3 may be related to the removal process of the planar fault during Li insertion. However, both diffraction patterns are missing {220} reflections whose intensity is supposed to be weak compared to the {440} reflections. Since the {220} peaks represent cation occupancy of the tetrahedral 8a sites,[25] its absence is indicative of the distorted spinel structure after the cycling.

The TEM study of $Li_{0.7}[Ni_{1/6}Mn_{5/6}]O_2$ indicates that the as-prepared material is highly faulted with a new type of directional planar fault that is unstable against the electrochemical cycling. Although we cannot explain how such fault improves the capacity fade exhibited by the normal spinel $LiMn_2O_4$ material, the $Li_{0.7}[Ni_{1/6}Mn_{5/6}]O_2$ produced through the ion-exchange process represents a new type of defective spinel structure with unique electrochemical property.

Conclusions

$Li_{0.7}[Ni_{1/6}Mn_{5/6}]O_2$ has been prepared by ion exchange of Li for Na in $Na_{0.7}[Ni_{1/6}Mn_{5/6}]O_2$ precursor synthesized by a sol-gel method using glycolic acid as a chelating agent. The material consists of a new type of defective spinel structure and shows good cycling behavior, retaining 98% (0.0486 mAh/g·cycle) of the initial capacity after 50 cycles. Close examination of the powder structure using TEM revealed that the as-prepared powder was highly faulted with planar faults, which appears to be removed by the electrochemical cycling. The synthesis of the material and the electrochemical property of the material was quite reproducible. Further detailed investigation is underway in order to determine the mechanism for the formation of such highly directional planar faults and its effects on the cycling behavior.

Hanyang University assisted in meeting the publication costs of this article.

References

1. M. M. Thackeray, P. G. David, P. G. Bruce, and J. B. Goodenough, *Mater. Res. Bull.*, **18**, 461 (1983).
2. T. Ohzuka, M. Kitagawa, and T. Hirai, *J. Electrochem. Soc.*, **137**, 769 (1990).
3. A. Yamada, K. Miura, K. Hinokuma, and M. Tanaka, *Mater. Res. Bull.*, **142**, 2149 (1995).
4. R. J. Gummow, A. de Kock, and M. M. Thackeray, *Solid State Ionics*, **69**, 59 (1994).
5. K. Amine, H. Tukamoto, H. Yasuda, and Y. Fujita, *J. Electrochem. Soc.*, **143**, 1607 (1996).
6. D. Guyomard and J. M. Tarascon, *Solid State Ionics*, **69**, 222 (1994).
7. G. G. Amatucci, C. N. Schmutz, A. Bylr, C. Siala, A. S. Gozdz, D. Larcher, and J.-M. Tarascon, *J. Power Sources*, **69**, 11 (1997).
8. Y. Xia, Y. Zhou, and M. Yoshio, *J. Electrochem. Soc.*, **144**, 2593 (1997).
9. H. Huang, C. A. Vincent, and P. G. Bruce, *J. Electrochem. Soc.*, **146**, 481 (1999).
10. A. R. Armstrong and P. G. Bruce, *Nature (London)*, **381**, 499 (1996).
11. F. Captaine, P. Gravereau, and C. Delmas, *Solid State Ionics*, **89**, 197 (1996).
12. G. Vitins and K. West, *J. Electrochem. Soc.*, **144**, 2587 (1997).
13. A. R. Armstrong, A. D. Robertson, and P. G. Bruce, *Electrochim. Acta*, **45**, 285 (1999).

14. J. N. Reimers, E. W. Fuller, E. Rossen, and J. R. Dahn, *J. Electrochem. Soc.*, **140**, 3396 (1993).
15. I. J. Davidson, R. J. McMillan, J. J. Murray, and J. E. Greedan, *J. Power Sources*, **54**, 232 (1995).
16. L. Croguennec, P. Deniard, and R. Brec, *J. Electrochem. Soc.*, **144**, 3323 (1997).
17. Y.-I. Jang, B. Huang, Y.-M. Chiang, and D. R. Sadoway, *Electrochem. Solid-State Lett.*, **1**, 13 (1998).
18. J. M. Paulsen, C. L. Thomas, and J. R. Dahn, *J. Electrochem. Soc.*, **146**, 3560 (1999).
19. J. M. Paulsen, C. L. Thomas, and J. R. Dahn, *J. Electrochem. Soc.*, **147**, 861 (2000).
20. Z. Lu and J. R. Dahn, *J. Electrochem. Soc.*, **148**, A237 (2001).
21. J. M. Paulsen, R. A. Donaberger, and J. R. Dahn, *Chem. Mater.*, **12**, 2257 (2000).
22. T. E. Quine, M. J. Duncan, A. R. Armstrong, A. D. Robertson, and P. G. Bruce, *J. Mater. Chem.*, **10**, 2838 (2000).
23. B. Ammundsen, J. Desilvestro, T. Groutso, D. Hassell, J. B. Metson, E. Regan, R. Steiner, and P. J. Pickering, *J. Electrochem. Soc.*, **147**, 4078 (2000).
24. J.-P. Parant, R. Olaszuaga, M. Devalette, C. Fouassier, and P. Hagenmuller, *J. Solid State Chem.*, **3**, 1 (1971).
25. H. Wang, Y. I. Jang, and Y. M. Chiang, in *Proceedings of the Symposium on Processing and Characterization of Electrochemical Materials and Devices*, Vol. 109, p. 297, American Ceramic Society, Cincinnati, OH (2000).